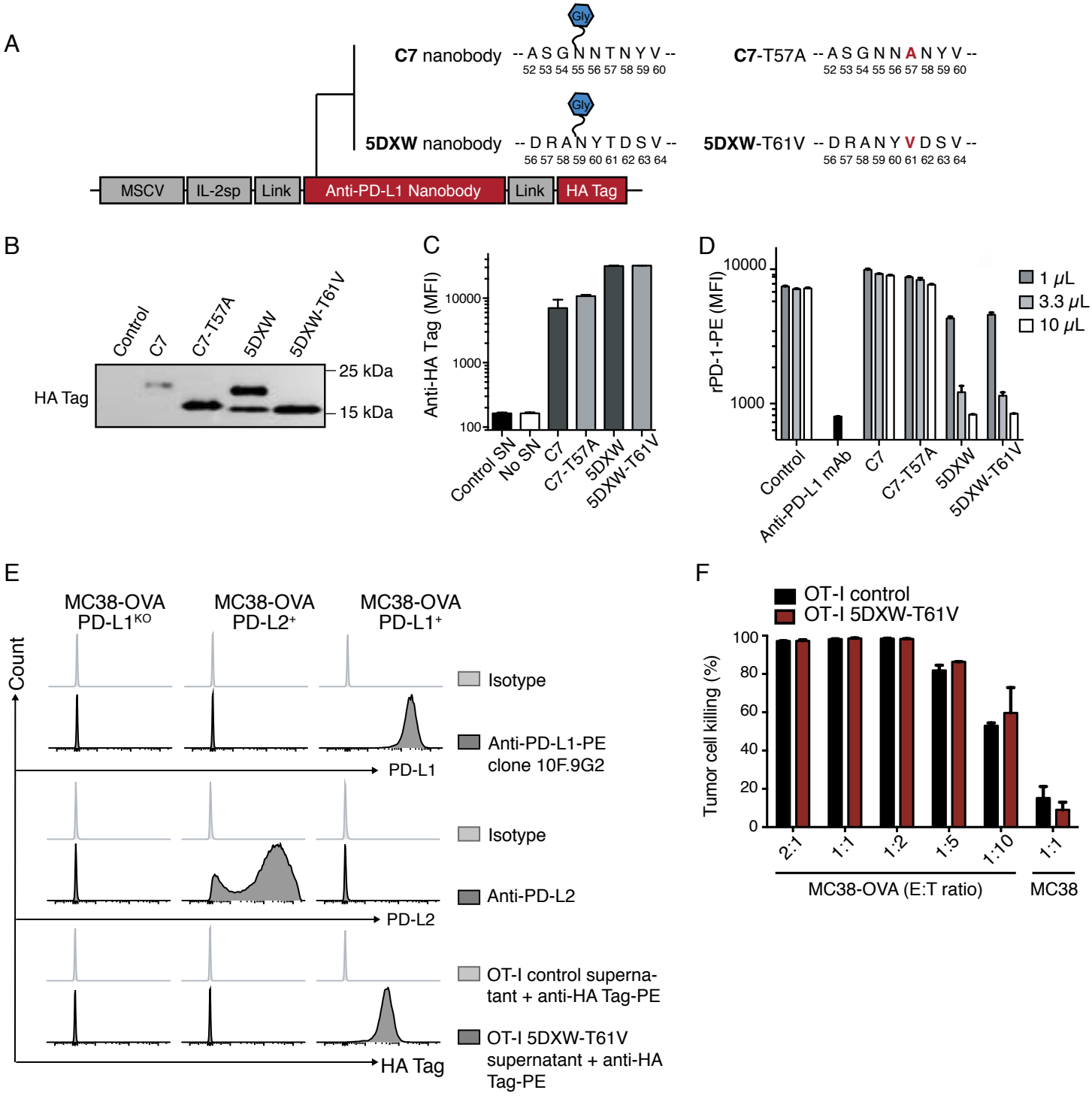

Supplementary Figure S1. *In vitro* evaluation of anti-PD-L1 nanobodies and nanobody-secreting T cells
(A) Illustration of the N-Glycosylation site in C7 and 5DXW nanobodies amino acid sequences. Designed non-glycosylated mutants are displayed on the right. **(B)** Western blot analysis on supernatant from HEK 293T cells transfected with retroviral vectors containing the four different nanobodies. The data shown are representative of 2 experiments. **(C)** Binding capacity of produced nanobodies. B16-OVA PD-L1$^+$ cells were incubated with supernatant from nanobody-transfected HEK 293T cells or control HEK 293T cells, then stained with an anti-HA Tag antibody and analyzed by flow cytometry. The data shown are mean ± SEM pooled from 2 independent experiments, n=2. **(D)** Blocking capacity of produced nanobodies. B16-OVA PD-L1$^+$ tumor cells were incubated with supernatant from non-transfected cells, nanobody-transfected cells or with blocking anti-PD-L1 antibody (clone 10F.9G2, 10 µg/ml, black bar) and stained with recombinant PD-1 PE (rPD-1 PE). The data shown are mean ± SEM pooled from 2 independent experiments. **(E)** Specificity of 5DXW-T61V nanobody for PD-L1. Flow cytometry plots on engineered MC38-OVA cells lines using anti-PD-L1, anti-PD-L2, or isotype antibody. For nanobody detection, cells were incubated with supernatant from OT-I control or OT-I 5DXW-T61V T cells and stained with anti-HA Tag antibody. The data shown are representative of 2 experimental replicates. **(F)** Killing of MC38-OVA PD-L1$^+$ or MC38 tumor cells by 5DXW-T61V nanobody-secreting or control OT-I cells after 24h of co-culture at different E:T ratios. The data shown are mean ± SEM, n=3 per condition. Data shown are representative of 2 experiments.

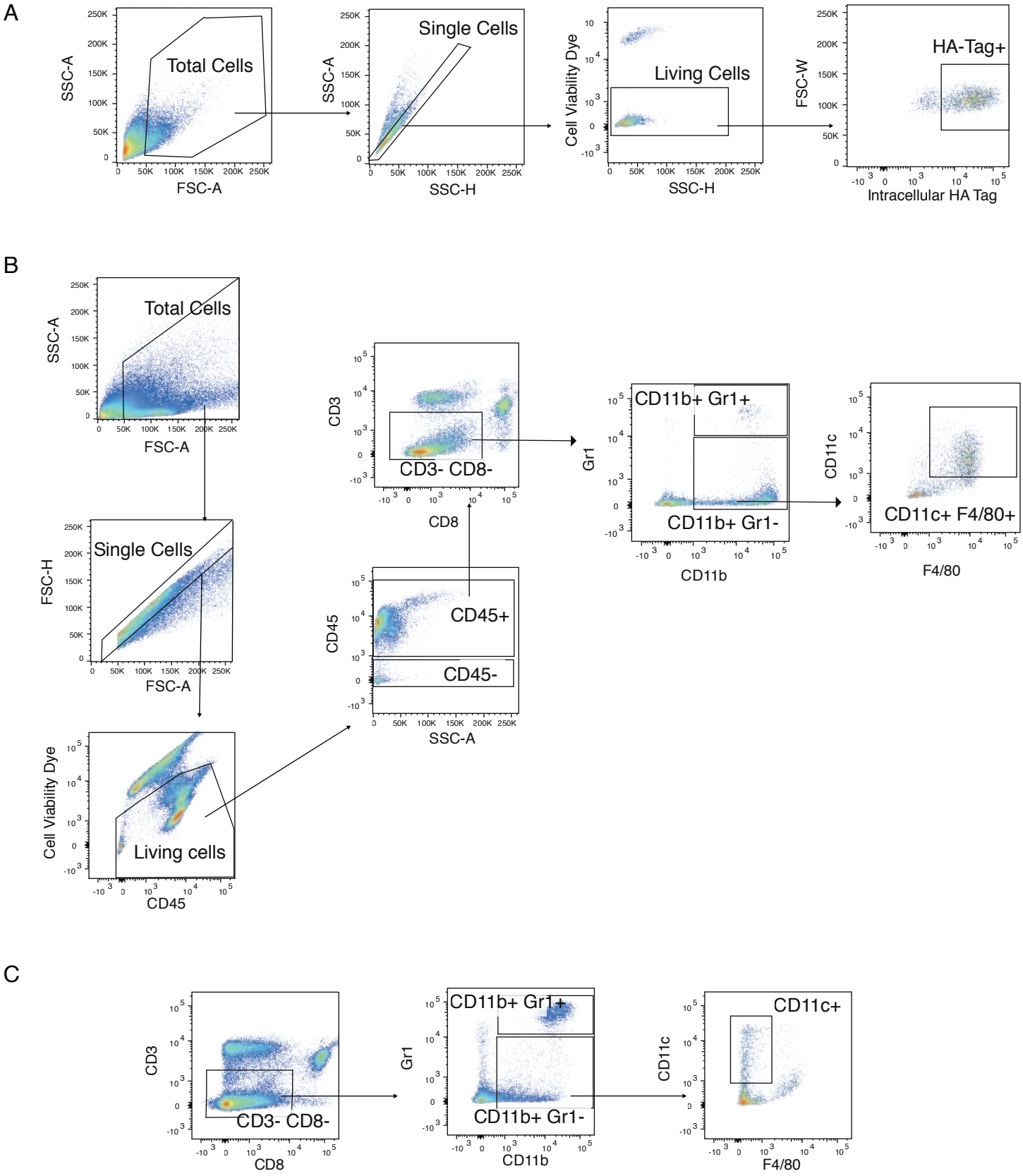

Supplementary Figure S2. Gating strategies used to evaluate the proportion of nanobody-producing T cells *in vitro* (A) and to identify macrophages and MDSCs populations from mouse samples (B-C).
(A) Analysis performed on OT-I T cells at day seven, after transduction with MSCV-5DXW-T61V plasmid at day two. Cells were selected using forward (FSC) and side scatters (SSC) detectors. Subsequently, we gated on single cells then on living cells. Intracellular HA Tag^{+} cells were considered as nanobody-producing OT-I T cells. Arrows show the sequence of the gating used. **(B)** Total cells from a tumor sample were selected using forward (FSC) and side scatters (SSC) detectors. Subsequently, we gated on single cells then on living cells, followed by identification of CD45^{+} and CD45^{-} cells. CD3^{-}CD8^{-} cells were identified from CD45^{+} cell population, followed by gating on CD11b^{+} Gr1^{+} (MDSCs) or CD11b^{+} Gr1^{-} cells. CD11c^{+} F4/80^{+} cells (Tumor macrophages) were further identified from CD11b^{+} Gr1^{-} cells. **(C)** The same strategy was applied for spleen and lymph nodes samples, but macrophages were identified as CD11c^{+} from CD11b^{+} Gr1^{-} cells. Representative of the subsequent gating on CD3^{-}CD8^{-} cells on a spleen sample.

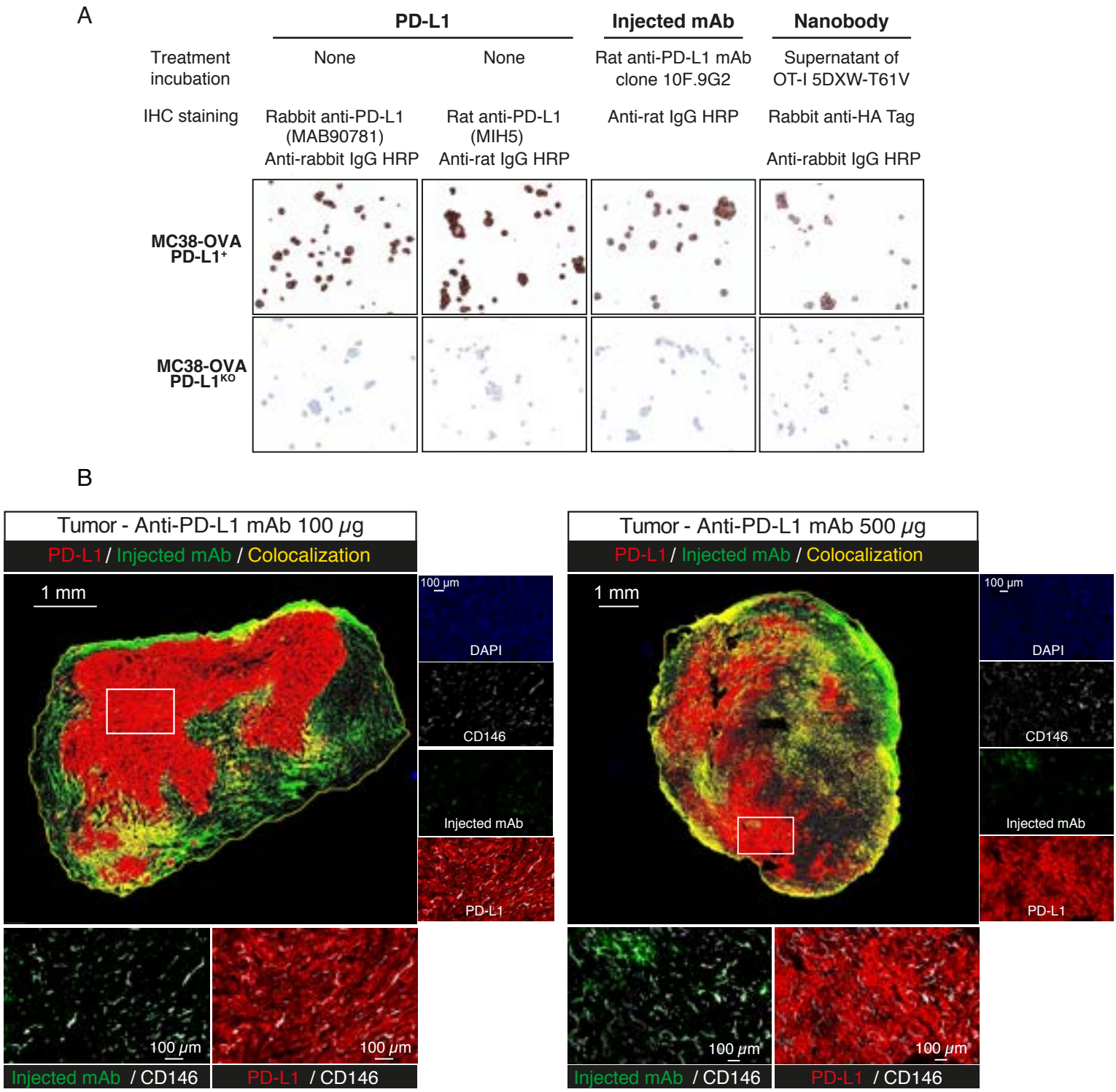
A
PD-L1
Injected mAb
Nanobody
Treatment incubation
None
None
Rat anti-PD-L1 mAb clone 10F.9G2
Supernatant of OT-I 5DXW-T61V
IHC staining
Rabbit anti-PD-L1 (MAB90781)
Anti-rabbit IgG HRP
Rat anti-PD-L1 (MIH5)
Anti-rat IgG HRP
Anti-rat IgG HRP
Rabbit anti-HA Tag
Anti-rabbit IgG HRP
MC38-OVA PD-L1+
MC38-OVA PD-L1KO
B
Tumor - Anti-PD-L1 mAb 100 µg
PD-L1 / Injected mAb / Colocalization
Tumor - Anti-PD-L1 mAb 500 µg
PD-L1 / Injected mAb / Colocalization
1 mm
100 µm
DAPI
CD146
Injected mAb
PD-L1
Injected mAb / CD146
PD-L1 / CD146
C
%age of PD-L1 area covered by treatment (injected mAb/Nanobody)
***
***
100 µg
500 µg
Injected anti-PD-L1 mAb
ACT OT-I 5DXW-T61V (Nanobody)
D
PD-L1+ area (%age of total area)
ns
ns
100 µg
500 µg
Injected anti-PD-L1 mAb
ACT OT-I 5DXW-T61V (Nanobody)

Supplementary Figure S3. Increasing injection dose cannot overcome poor tumor penetration of injected anti-PD-L1 antibody

(A) Validation of IHC antibodies. MC38-OVA PD-L1^{+} or PD-L1KO tumor cells were incubated with PBS, anti-PD-L1 monoclonal antibody ('injected mAb', clone 10F.9G2) or supernatant from 5DXW-T61V-secreting OT-I T cells. Cell pellets were then frozen in O.C.T. compound and cut in 6 µm sections. Detection of total PD-L1, injected mAb and HA-Tagged nanobody on frozen sections was performed with indicated primary and secondary antibodies. Staining was revealed with DAB. **(B-D)** Tumor penetration of injected anti-PD-L1 mAb. MC38-OVA tumor-bearing mice were treated with anti-PD-L1 monoclonal antibody (100 µg or 500 µg *i.p.* on day 0 and day 4) or ACT of 5DXW-T61V-secreting OT-I T cells (10 x 10^6 cells *i.v.* injection at day 0). Mice were sacrificed and tumors were collected for IF analysis on day 7. **(B)** Colocalization (in yellow) of total PD-L1 staining and injected mAb staining was visualized with HALO software after IF processing of tumor samples. Areas where only PD-L1 was detected appear in red, and areas where only injected mAb was detected appear in green. Bottom panels: IF images of the same tumors at higher magnification. Anti-CD146 antibody staining of endothelial cells appears in white. The data shown are representative of 6 samples per group. **(C)** Comparison of PD-L1/injected mAb and PD-L1/nanobody colocalization areas in the tumor from mice treated with injected mAb or ACT of nanobody-secreting T cells. The data shown are calculated as a percentage of co-stained surface area over total PD-L1-stained surface area for each tumor sample, mean ± SEM, n=6. An unpaired t-test was used to determine statistical significance. ACT OT-I 5DXW-T61V vs anti-PD-L1 mAb 100 µg, *** p=0.0009, ACT OT-I 5DXW-T61V vs anti-PD-L1 mAb 500 µg, *** p=0.0004. Total PD-L1 expression in tumors was not significantly different between treatment groups **(D)**.

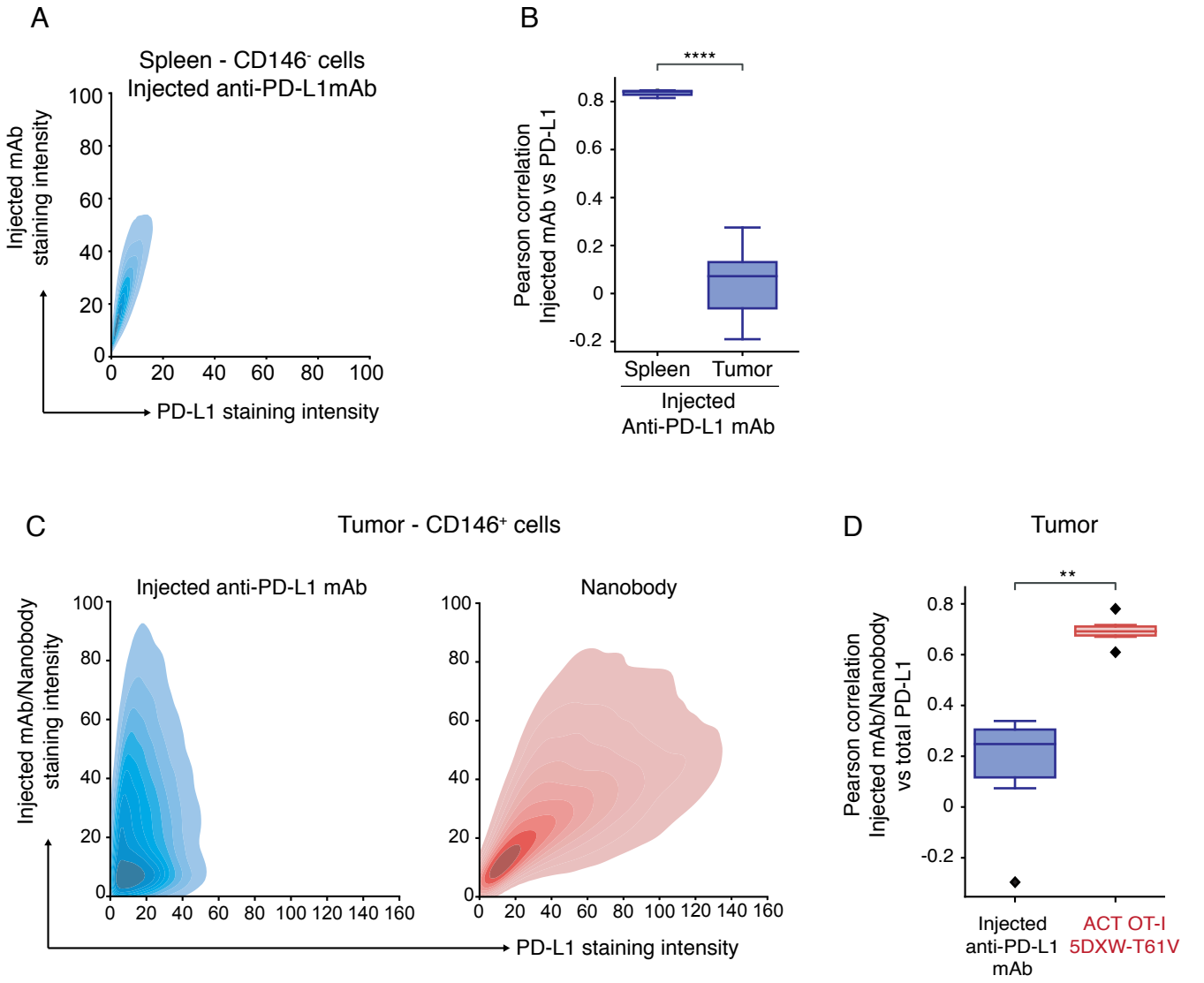

Supplementary Figure S4. Staining correlations in the spleen and on CD146⁺ cells in the tumor
MC38-OVA tumor-bearing mice were treated with anti-PD-L1 monoclonal antibody ('injected mAb') or ACT of 5DXW-T61V-secreting OT-I T cells. Tumor and spleen samples were collected after seven days for IF stainings of PD-L1, injected mAb and nanobody. **(A)** Kernel density estimation plot representing the correlation between PD-L1 staining and injected mAb staining intensities on individual non-endothelial cells (CD146⁻) from spleens of mice treated with anti-PD-L1 antibody. 615,511 cells were identified from 3 spleens. **(B)** Boxplot representing the Pearson correlation between PD-L1 staining and injected mAb staining intensities over all non-endothelial cells in spleen and tumor samples from anti-PD-L1 antibody-treated mice. A highly significant difference in the correlation of staining intensities was found between spleen and tumor from anti-PD-L1 antibody-treated mice. Spleen, n=3. Tumor, n=6. Pairwise contrasts between correlations were calculated using Welch's t-test, **** $p<0.0001$. **(C)** Kernel density estimation plots representing the correlation between PD-L1 staining intensity and injected mAb or nanobody staining intensity on individual endothelial cells (CD146⁺) for all biological replicates. 135,649 cells were identified from 6 samples of mice treated with anti-PD-L1 antibody (left panel) and 72,966 cells were identified from 6 mice treated with ACT of OT-I 5DXW-T61V-secreting T cells (right panel). **(D)** Boxplot representing the Pearson correlation between PD-L1 staining intensity and injected mAb or nanobody staining intensity over all CD146⁺ cells from tumor samples of indicated treatment groups. Pairwise contrasts between correlations were calculated using Welch's t-test. Correlation between PD-L1 and nanobody is significantly better than correlation between PD-L1 and injected mAb. Black squares represent outliers. ** $p=0.00230$. **(C-D)** The data shown are pooled from 2 experiments.

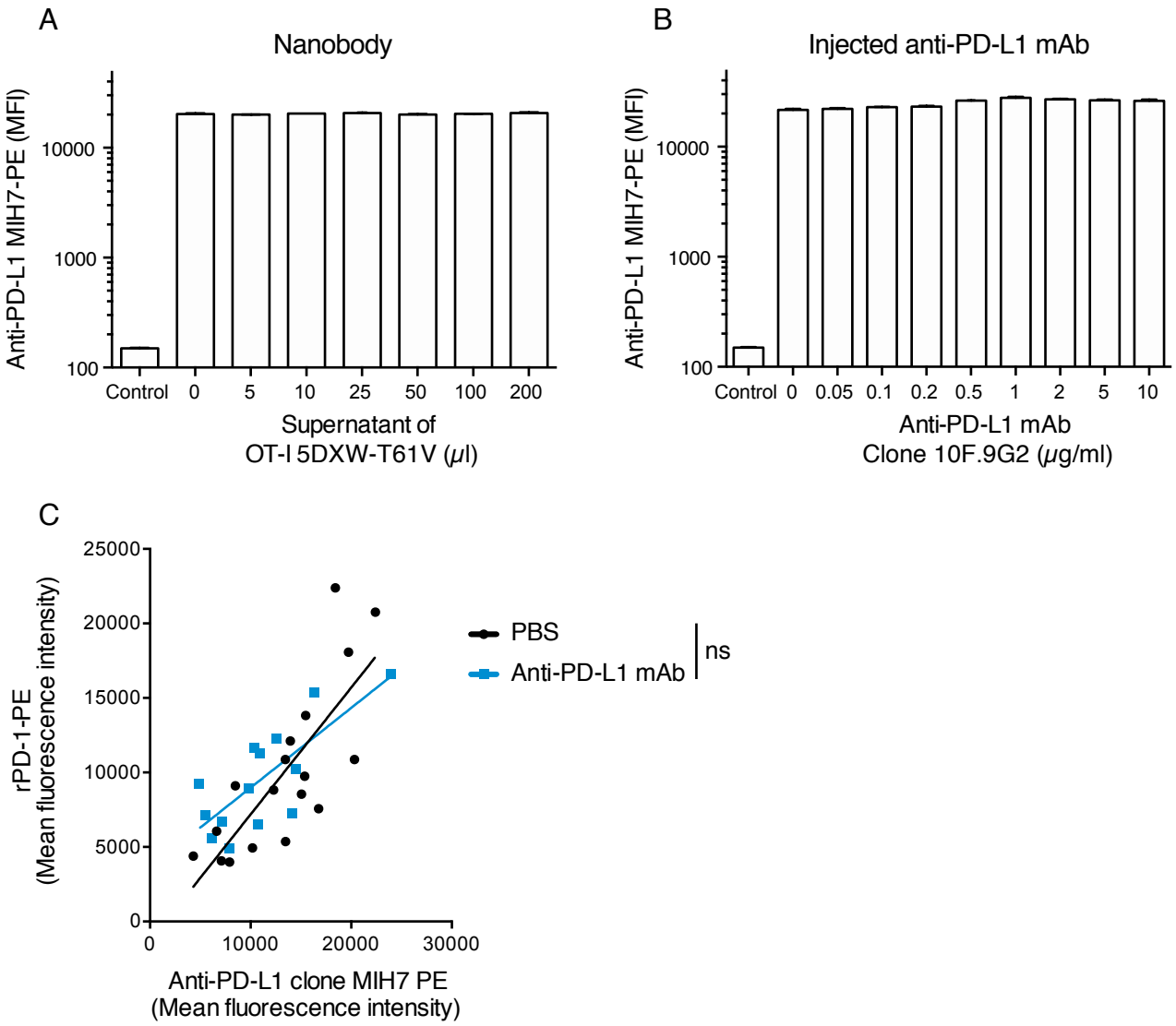

Supplementary Figure S5. Limited intratumoral penetration of injected anti-PD-L1 mAb revealed by a high level of rPD-1 binding to free PD-L1 in the tumor

(A-B) Anti-PD-L1 antibody (clone MIH7) was chosen to assess total PD-L1 level since its binding is not influenced by the presence of 5DXW-T61V nanobody or anti-PD-L1 antibody clone 10F.9G2 ('injected mAb'). MC38-OVA PD-L1$^+$ cells were incubated with increasing amounts of supernatant from 5DXW-T61V-secreting OT-I T cells **(A)** or an increasing concentration of injected mAb. **(B)** Cells were then stained with anti-PD-L1 clone MIH7 coupled to PE. Unstained cells were used as a control to indicate the baseline fluorescence level. The data shown are mean ± SEM, n=2. **(C)** MC38-OVA tumor-bearing mice were treated with PBS or injected mAb. Tumors were collected after 7 days and cell suspensions from tumor samples were split in two and stained either with rPD-1-PE or anti-PD-L1-PE (clone MIH7). Correlation between the MFI of rPD-1-PE and the MFI of anti-PD-L1 (MIH7) PE on CD11b$^+$F4/80$^+$ or CD11b$^+$ Gr1$^+$ cells were shown in a scatterplot. Gating strategy is illustrated in Suppl. Fig. S2B. Each dot represents one of the two myeloid populations from one sample. n=7-9, samples were pooled from two independent experiments. Linear regression slopes were compared with ANCOVA to determine significance, ns p=0,169.

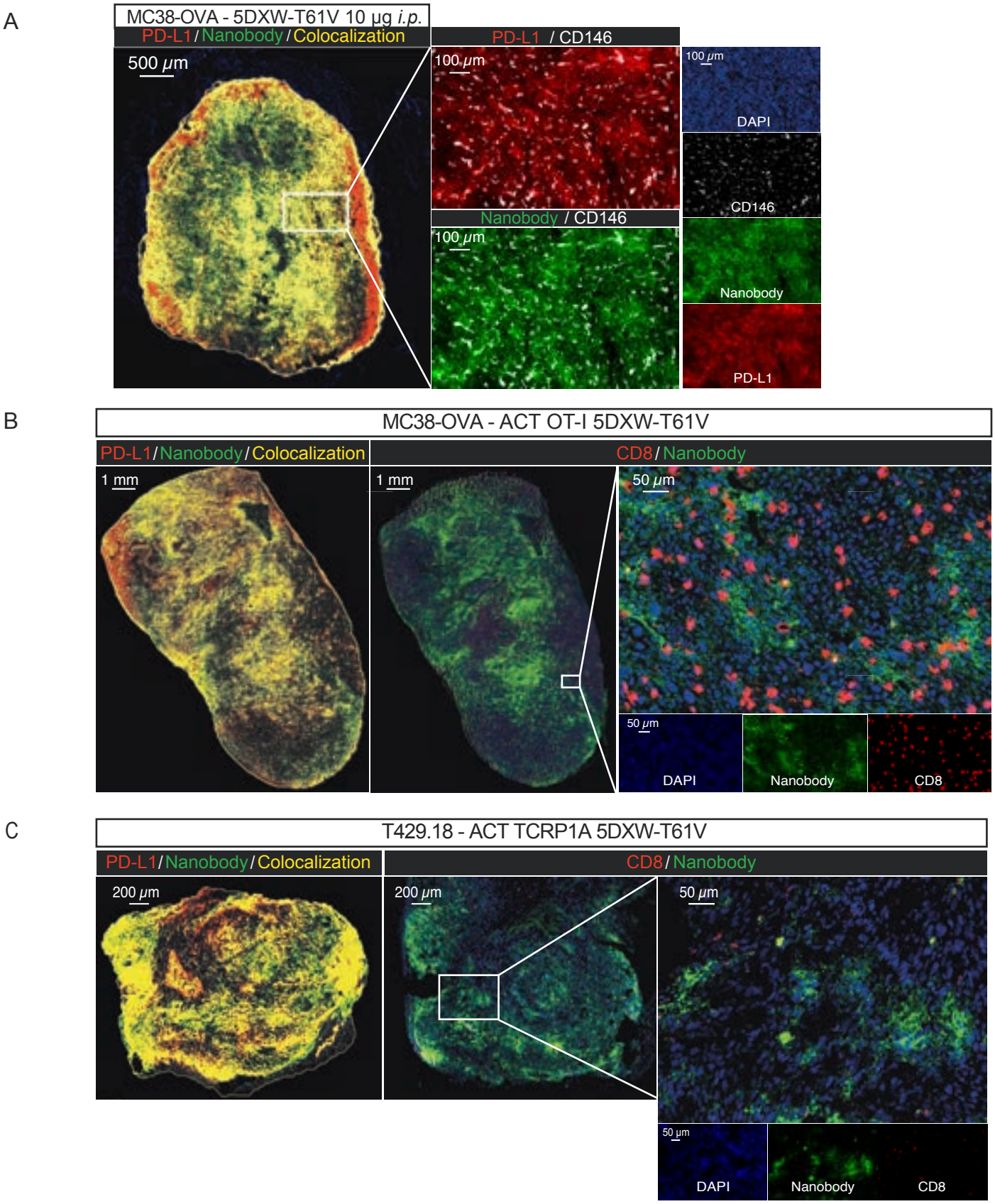

Supplementary Figure S6. Intratumoral nanobody penetration following systemic injection or ACT of nanobody-secreting CD8 T cells

(A) Intratumoral penetration of anti-PD-L1 nanobody after systemic injection. MC38-OVA tumor-bearing mice were injected *i.p.* with 10 µg of purified 5DXW-T61V nanobody. Mice were sacrificed after 1h, and tumor samples were collected for IF analysis. Colocalization (in yellow) of PD-L1 and nanobody was visualized with HALO software (**left panel**). Areas where only PD-L1 was detected appear in red, and areas where only nanobody was detected appear in green. **Right panels:** IF images at higher magnification. Anti-CD146 antibody staining of endothelial cells appears in white. The data shown are representative of 5 samples. **(B,C)** Nanobody-secreting CD8 T cell distribution in tumors upon adoptive cell transfer. MC38-OVA and T429.18 tumor-bearing mice were treated with ACT of 5DXW-T61V-secreting OT-I T cells **(B)** or 5DXW-T61V-secreting TCRP1A CD8 T cells **(C)**, respectively. Seven days after ACT, tumor samples were collected for IF analysis. **Left panels:** Colocalization (yellow) of nanobody (green) and PD-L1 (red) in a MC38-OVA tumor **(B)** or in a T429.18 tumor after treatment **(C)**, visualized by HALO software. **Right panels:** Nanobody-secreting CD8 T cells appear in yellow, the distribution of secreted anti-PD-L1 nanobody appears in green, and bystander T cells appear in red.

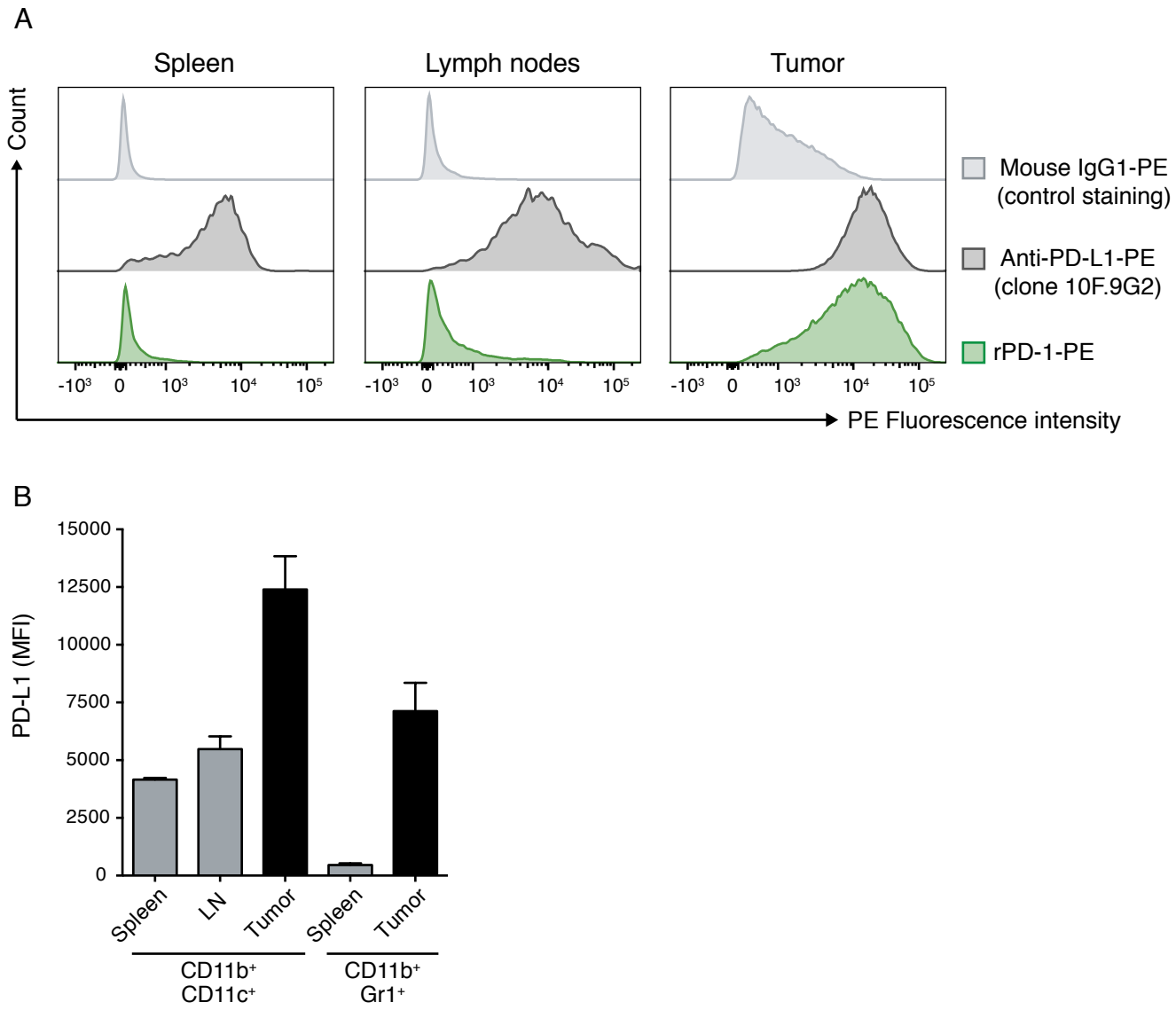

Supplementary Figure S7. Recombinant PD-1 binding and PD-L1 detection on myeloid cells in the tumor and in secondary lymphoid organs

Spleen, lymph nodes, and tumor samples from MC38-OVA tumor-bearing mice were collected after 7 days for flow cytometry analysis. **(A)** Flow cytometry plots representing PD-L1 detection (using anti-PD-L1-PE antibody clone 10F.9G2) or recombinant PD-1 binding (using rPD-1-PE) on $CD45^+CD11b^+CD11c^+$ cells from the spleen, lymph nodes (LN) or tumor. Mouse IgG1-PE isotype staining was used as a staining control. **(B)** Evaluation of PD-L1 expression on myeloid cells in the spleen, LN or tumor by flow cytometry. Median fluorescence intensity of anti-PD-L1-PE staining on $CD45^+CD11b^+CD11c^+$ or $CD45^+CD11b^+$ $Gr1^+$ cells. Gating strategy is illustrated in Suppl. Fig. S2B. A higher PD-L1 expression is found in the tumor. The data shown are mean ± SEM, n=5. Representative of 2 experiments.

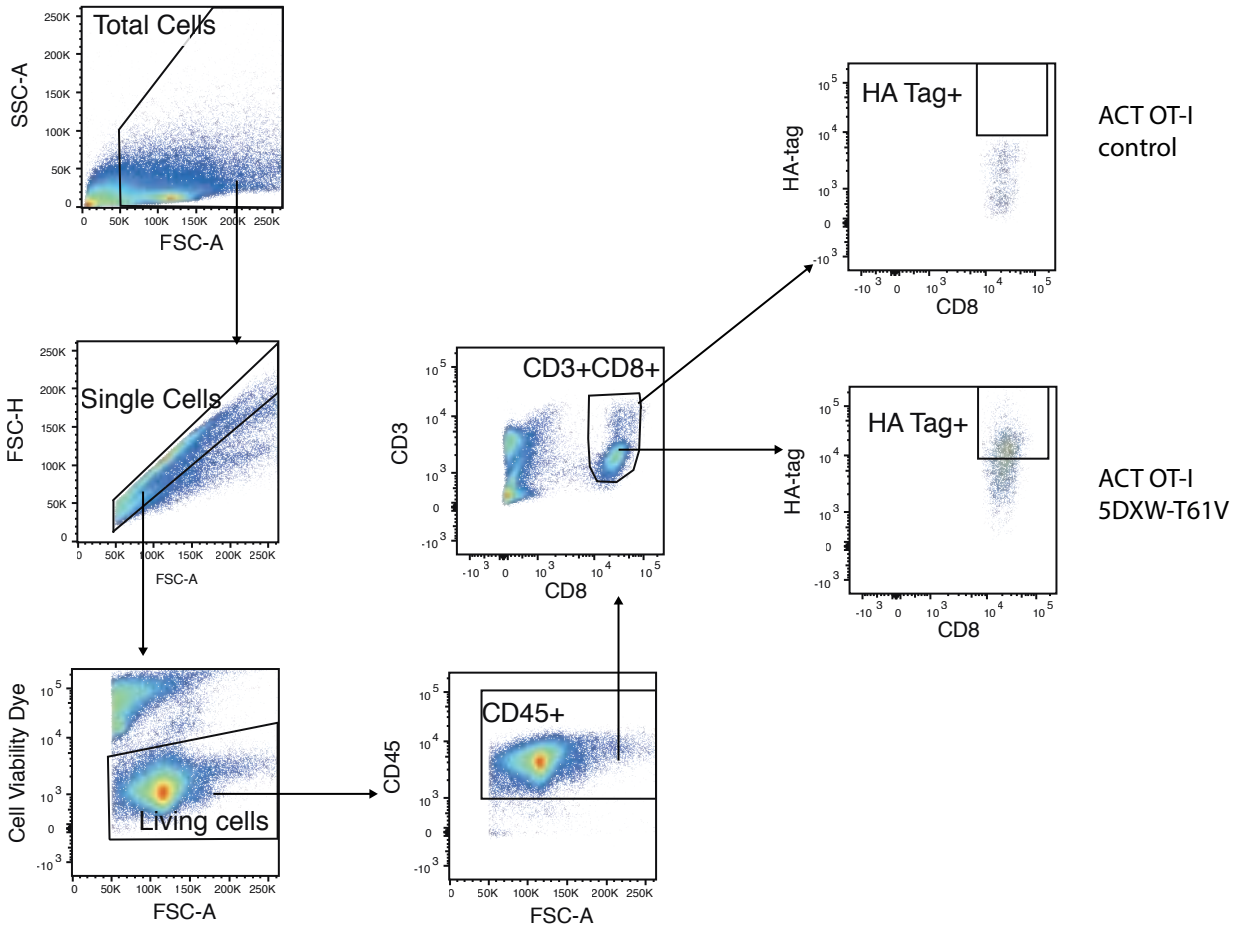

Supplementary figure S8. Gating strategy used to evaluate the proportion of nanobody-producing T cells *in vivo.*
Total cells from a tumor sample were selected using forward (FSC) and side scatters (SSC) detectors. Subsequently, we gated on single cells then on living cells, followed by identification of $CD45^+$ cells. $CD3^+CD8^+$ cells were sub-gated from $CD45^+$ cell population. Intracellular HA Tag signal in $CD3^+CD8^+$ cells from a tumor-bearing mouse treated with ACT of control OT-I T cells was used to set the threshold for positive cells.

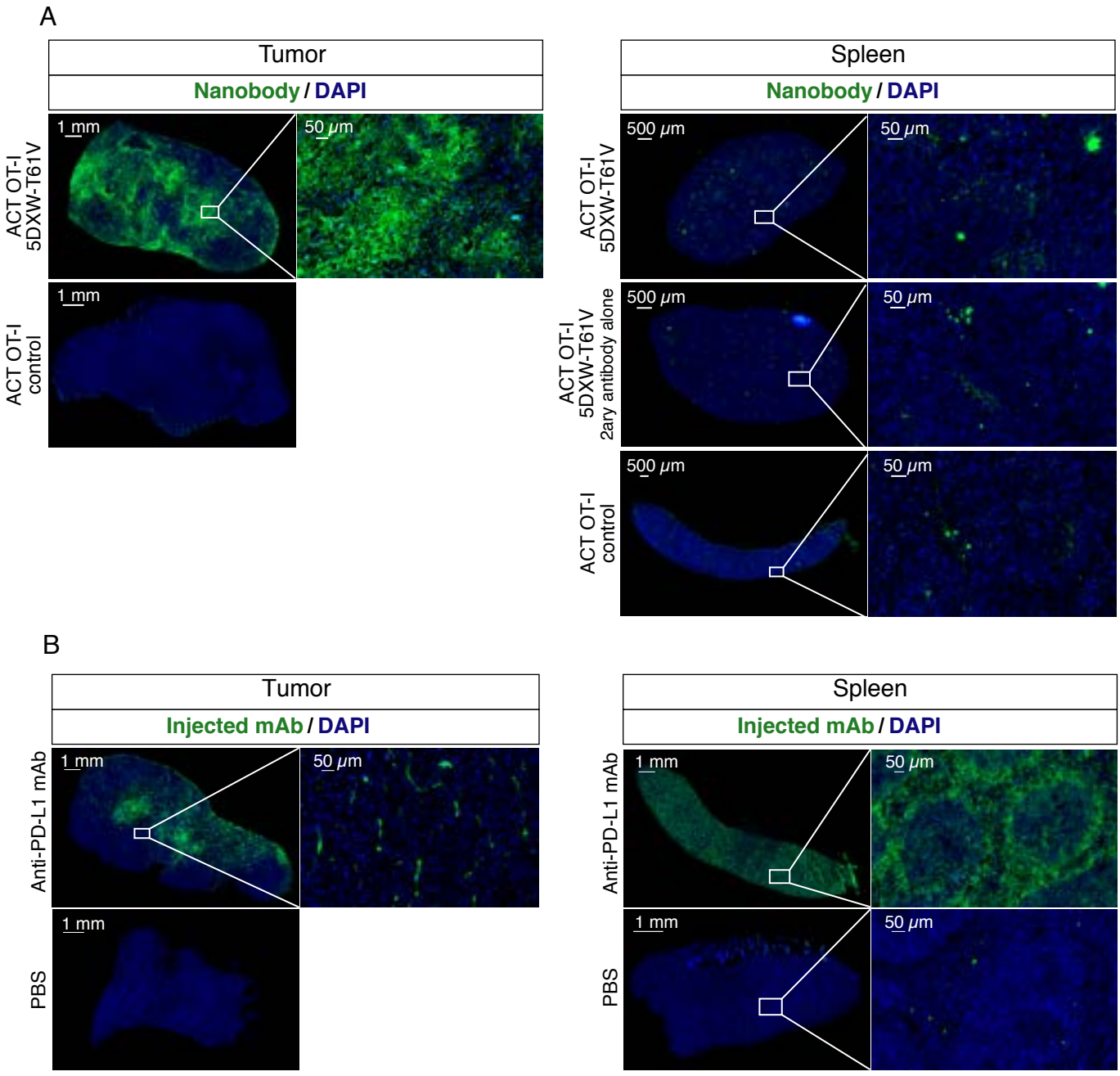

Supplementary Figure S9. Distribution of secreted nanobody and injected mAb in tumors and spleens of treated mice

(A) Nanobody distribution in tumor and spleen samples from mice treated with ACT of 5DXW-T61V-secreting or control OT-I T cells. Nanobody (anti-HA Tag staining) appears green, and nuclei appear blue. Secreted nanobody was detected in the tumor **(left panel)** but not in the spleen **(right panel)**. Only a background staining could be detected in the spleen, at a level similar to the spleen from mice that received control ACT or to the anti-rabbit IgG HRP secondary antibody control. **(B)** Injected mAb distribution in tumor and spleen samples from mice treated with anti-PD-L1 antibody ('injected mAb') or PBS. Injected mAb appears in green, and nuclei appear in blue. Conversely to locally secreted anti-PD-L1 nanobody, the injected mAb was mainly found in the spleen **(right panel)** and is only detectable in certain areas in the tumors **(left panel)**.

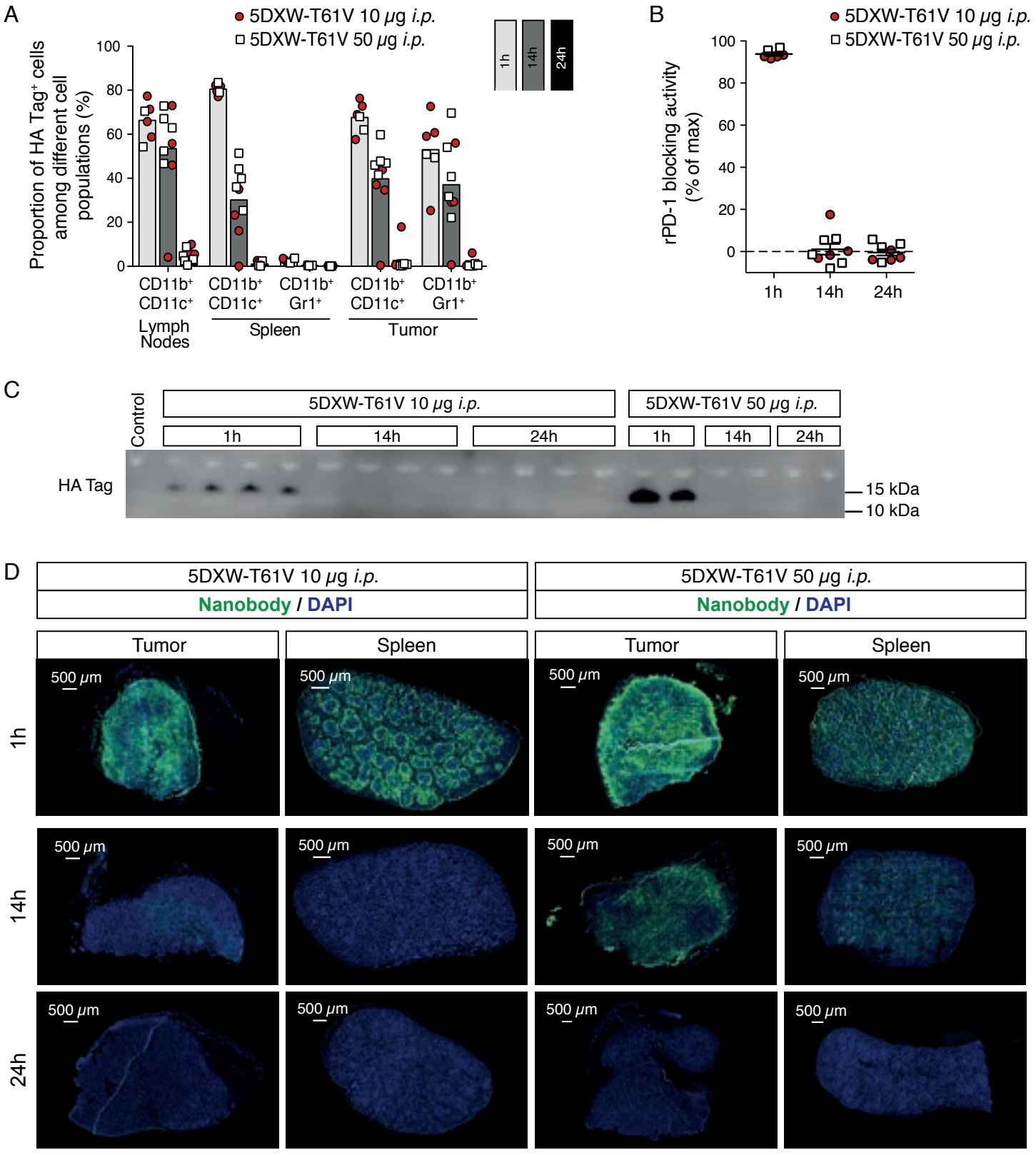

Supplementary Figure S10. Nanobody distribution after systemic injection

MC38-OVA tumor-bearing mice were injected *i.p.* with 10 µg or 50 µg of purified 5DXW-T61V nanobody. Mice were sacrificed after 1h, 14h, or 24h, and serum, lymph nodes, spleen, and tumor samples were collected. **(A)** Percentage of cells bound by anti-PD-L1 nanobody among myeloid cell populations in the lymph nodes, spleen and tumor of injected mice, as detected by surface staining with anti-HA Tag antibody using flow cytometry. Each dot represents one mouse sample, and columns represent mean values for each time point. 10 µg, n=4; 50 µg, n=2-5. Gating strategy is illustrated in Suppl. Fig. S2B. **(B)** Abundance of anti-PD-L1 nanobody in the serum of treated mice. MC38-OVA PD-L1$^+$ cells were incubated with 20 µl sera from purified 5DXW-T61V nanobody-treated mice before staining with recombinant PD-1-PE (rPD-1-PE). rPD-1 blocking activity is calculated as the reduction of rPD-1-PE median fluorescence intensity with sera from treated mice as compared to sera from PBS-treated mice. The data shown are mean ± SEM. 10 µg, n=4; 50 µg, n=2-5. **(C)** Western blot analysis on the sera from purified 5DXW-T61V nanobody-treated mice. The serum from a PBS-treated mouse is loaded as a control. **(D)** IF analysis representing the detection of purified 5DXW-T61V nanobody upon systemic injection after different time points. Nanobody (anti-HA Tag staining) appears green, and nuclei appear blue.